Phase Transitions in Strontium Titanate

Xinyue Fang

Department of Physics, University of Illinois at Urbana-Champaign

Abstract

Strontium Titanate $SrTiO_3$ (STO) is known to undergo an antiferrodistortive transition from cubic to tetragonal phase at $T_c \approx 105K$, and classical to quantum paraelectric phase transition at $T_q \approx 37K$. This paper is intended to use Landau Theory to explore these two phase transitions of STO, as well as some experimental techniques to examine this model.

1   Introduction

Strontium Titanate, $SrTiO_3$ (STO) is a complex oxide material with per-ovskite structure. It has attracted particular attention because of its potential use in modern electronic devices. STO is a potential ferroelectric material material in which the ferroelectric transition is suppressed by quantum fluctuation. At $T_q \approx 37K$, the STO crystal experiences a quantum transition from classical to quantum paraelectric state [1]. As the temperature continuously increases, a structural phase transition from low temperature tetragonal phase (point group 4/mmm) to high temperature cubic phase (point group m3m) is observed in the crystal at $T_c \approx 105K$.

During the past few years, STO has been studied thoroughly by Raman spectroscopy, X-ray, and neutron diffraction. In particular, optical scattering studies at $T < T_q$ showed that the structure of central peak became more complex than at the high temperature regions[2]. This peak contains several components which are forbidden by selection rules. X-ray and Neutron diffraction also show that the structural phase transition at T_c is close to second order transitions and is caused by softening of the transverse optical mode at R point. This phase transition has a great historical significance because every development in the theory of structural phase transitions measured its success on the ability to correctly describe experimental observations in STO.

2   Theory

Like most complex oxides with general formula ABO_3, STO has a simple cubic perovskite structure at room temperature, consisting of a simple cubic lattice of strontium atoms at corner, oxygen atoms at the face center, and titanium atoms at the body center, see Fig.1. The oxygen octahedral can easily rotate around the center titanium atom, giving rise to possible distortions to the perfect crystal[3].

2.1   Structural Phase Transition

At $T_c \approx 105K$, STO undergoes a cubic to tetragonal anti-ferrodistortive transition. This phase transition is from the rotation of the oxygen octahedral around one of the cubic main axes, and two adjacent cell rotate in the op-
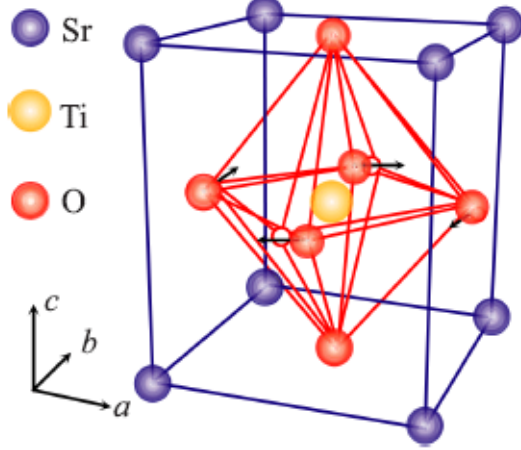
Figure 1: The crystal structure of STO

posite direction (Fig.2). Determine the temperature dependence of the free energy near this structural phase transition requires calculating the temperature dependence of the nonlinear susceptibilities[2]. In the Landau theory of phase transitions, the nonlinear susceptibility in the low temperature phase takes the form

$$\chi_{ijkl}^{Q4mmm} = \chi_{ijkl}^{Qm3m} + \triangle\chi_{ijkl}^{Q4mmm} \tag{1}$$

where

$$\triangle\chi_{ijkl}^{Q4mmm} = \theta_{ijklmn}\eta_m\eta_n \tag{2}$$

χ_{ijkl}^{Qm3m} is the nonlinear susceptibility, θ_{ijklmn} is the sixth rank tensor, both corresponding to high temperature phase, and η is the order parameter, which in the case for STO crystal, is the angle of oxygen octahedral rotation about the crystallographic axis[2]. The temperature dependence of the order parameter is determined by free energy, which takes the form

$$F_B = F_0 + \int dV \left(\frac{A}{2}\sum_{i=1}^{3}\eta_i^2 + \frac{D}{2}\sum_{i=1}^{3}(\triangledown\eta_i)^2 + \frac{B}{4}\left(\sum_{i=1}^{3}\eta_i^2\right) - \frac{B_1}{4}\sum_{i=1}^{3}\eta_i^4 \right) \tag{3}$$
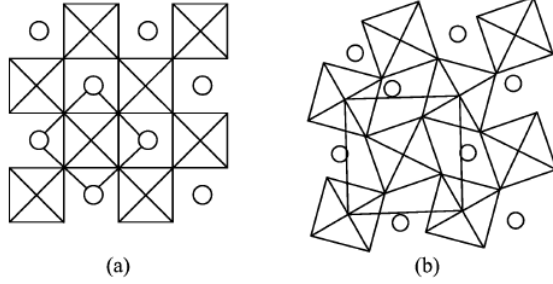
3

Figure 2: Schematic (001) face of STO crystal structure, showing TiO_6 octahedral and Sr^{2+} cations; (a)$T > 105K$, (b)$T < 105K$, with the rotation angle been greatly exaggerated

where

$$A = a(T - T_c), B > B_1 > 0 \qquad (4)$$

and a and D are the Landau expansion constants. For STO, $a = 5.4 \times 10^{-3} eV K^{-1}$ and $D = 3.7 \times 10^{-15} eV cm^2$[2].

It is known that $\eta = 0$ above T_c and $\eta \propto t^{1/2}$ below T_c, where $t = |T_c - T|/T_c$ is the reduced temperature. Therefore it follows that, below T_c the temperature dependence of the additional nonlinear susceptibility term is linear in temperature,

$$\triangle \chi_{ijkl}^{Q4mmm} \propto \alpha(T_c - T) \qquad (5)$$

where α is a constant. In the high temperature region where $T > T_c$, $\triangle \chi_{ijkl}^{Q4mmm} = 0$. The temperature dependence of χ_{ijkl}^{Qm3m} is unrelated to the phase transition, and can be included as a second order polynomial of the reduced temperature t. Therefore it follows that the temperature dependence of nonlinear susceptibility has a kink at $T = T_c$.

2.2 Quantum Paraelectric Phase Transition

Upon cooling, the dielectric constant of STO increase according to a Curie-Weiss law, $\epsilon = B + C/(T - T_c)$; however, on approaching $T_q = 37K$ from above, ϵ stabilizes at the value exceeding 10^4 and remains constant from $3K$ down to the lowest value $30mK$[1]. This property has been termed

4

a "quantum paraelectric state" by Muller and Burkard[4]. This quantum paraelectric-ferroelectric phase transition is influenced by coupled fluctuating phonon modes.

The soft mode optical phonon in ferroelectrics can be well described by a bosonic field theory[5]. The order parameter of this theory is the local polarization $\phi(x,t) = \sum_{i=1}^{n} e_i r_i(x,t)$, which is formally defined as one unit cell ar x containing n atoms of charge e_i, each individually displaced through r_i by the optic mode. As the optical mode softens, the action develops and instability and the order parameter must describe both quantum and thermal fluctuations. The action in three dimensional space can be expressed by Ginzburg-Landau phenomenology

$$
\begin{aligned}
S &= \int_0^{\beta} \{ \sum_{q,\alpha,\beta} [(\frac{a^2}{c^2}\partial_\tau^2 + a^2 q^2 + r + f q_\alpha^2)\delta_{\alpha\beta} \\
&\quad + (g - hq^2)\frac{q_\alpha q_\beta}{q^2}]\phi_\alpha(q)\phi_\beta(-q) \\
&\quad + \sum_{q,\alpha,\beta} (u + \nu\delta_{\alpha\beta})\phi_\alpha(q_1)\phi_\alpha(q_2)\phi_\beta(q_3)\phi_\beta(q_4)\}d\tau
\end{aligned}
\tag{6}
$$

Where a is the lattice constant, c is the speed of phonons, $q^2 = \sum_\alpha q_\alpha^2$, the dimensionless momenta $-\pi < q_\alpha < \pi$, and the second summation is carried out under the conservation of momemtum, $q_1 + q_2 + q_3 + q_4 = 0$. Since the field ϕ describes an electric dipole, the action includes long range dipole interation and also a coupling to the underlying lattice through the parameters r, f, g and h. The estimated values for the parameters are $r = 5.31$, $f = 55.7$, $g = 0.39$, and $h = 5.1$. The term u and ν describe local anharmonic interactions gives a net positive contribution, which ensures the polarization remain bounded. The mean-field phase diagram is sketched in Fig.3[5].

In the low temperature limit with the polarization aligned in one direction, we can integrate over quantum fluctuation to yield the free energy

$$
\begin{aligned}
F &= (r + \frac{g}{3})\phi^2 + u\phi^4 + \nu\sum_\alpha \phi_\alpha^4 \\
&\quad + \frac{3}{32\pi^2}[\pi\sqrt{\xi + \pi^2}(\xi + 2\pi^2) - \xi^2 ln(\frac{\pi}{\sqrt{\xi}} + \sqrt{1 + \frac{\pi^2}{\sqrt{\xi}}})] \\
&\quad + \frac{u^2\phi^2}{6\pi^2}[\frac{2\pi}{\sqrt{\xi + \pi^2}} - 2ln(\frac{\pi}{\sqrt{\xi}} + \sqrt{1 + \frac{\pi^2}{\xi}})]
\end{aligned}
\tag{7}
$$

5

with $\xi = r + 2(u + \mu)\phi^2 + 4u\phi^2/3$. This equation is found to be in good agreement with experimental results[5].
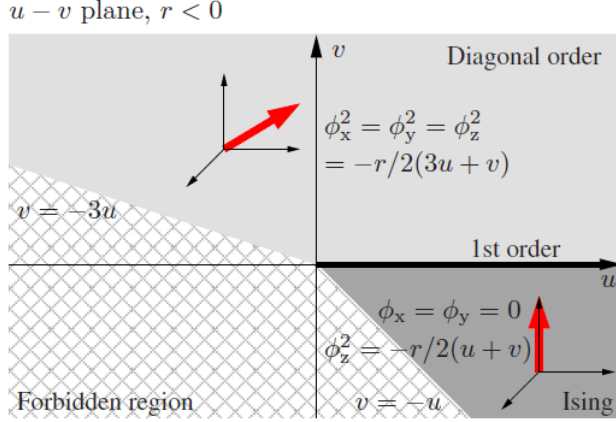

Figure 3: The phase diagram in the u-ν plane at zero temperature in the mean-field approximation. The crosshatched forbidden region denotes where the polarizibility would diverge without higher-order corrections. The solid thick line represents a first-order phase boundary between the light gray region that denotes diagonal order and the dark gray which labels the Ising phase. In each regime the inset axes illustrate the polarization solution highlighted by the bold vector.[5]

3 Experimental Techniques

The experiment of measuring the dielectric constant loss in STO crystal in a frequency range from $100Hz < \nu < 100MHz$ and temperature from $60K < T < 150K$ has been reported in ref[6]. The measurements were performed in home-built He-flow cryostat. All crystal in this experiment revealed the structural phase transition at $T_c = 105K$ as shown in fig.4.

Another way to examine the phase transitions in STO is elastic measurements on STO single crystal. The basic idea is that linear, harmonic mode coupling between the transverse optic (TO) soft phonon mode at wave vector q and the longitudinal acoustic (LA) mode at same q would depress the entire acoustic phonon branch, producing a decrease in LA

sound velocity. Fig.5(a) illustrates peaks in the longitudinal elastic coefficient $C_L = (1/2)(C_{11} + C_{12+2C_{44}})$, and Fig.5(b) shows C_{44}[7].
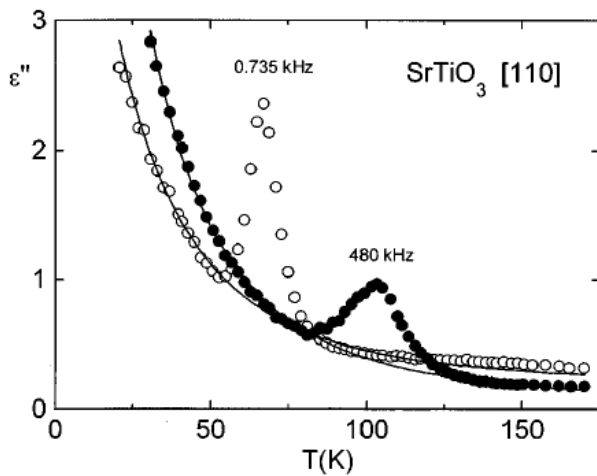

Figure 4: Temperature dependence of the dielectric loss in SrTiO3 at measuring frequencies of 735 Hz and 480 kHz. In the experimental setup the electric field was parallel to the [110] direction. The solid lines are spline fits to get an estimate of the frequency independent loss, on which the relaxation peaks are superimposed

Also a dielectric investigation on STO down to $0.3K$ shows the classical to quantum paraelectric phase transition at $T_q = 37K$[4]. Between $4K$ and $0.3K$, the dielectric constant ϵ is independent of temperature. ϵ does not vary below $4K$ is an evidence for occurrence of a quantum-mechanical regime which stabilizes large ferroelectric fluctuations in the paraelectric phase, as shown in Fig.6. phase.

The quantum phase transition can be examined by electron paramagnetic resonance of Fe^{3+}, which gives evidence for a classical to quantum phase transition in STO at $T_q = 37 \pm 1K$[1], both in tetragonal and pressure-induced trigonal phase.
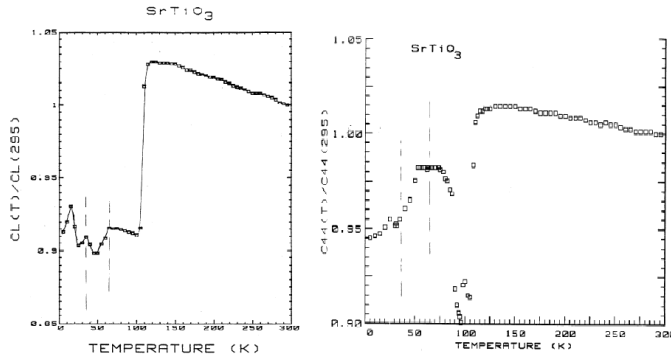

Figure 5: (a)Longitudinal elastic constant CL in strontium titanate versus temperature, normalized to unity at $295K$. Maximum is observed at the $106.5K$; (b) C_{44} shear coefficient in STO. A sharp dip is observed at $106.5K$

4   Conclusion

In summary, both cubic to tetragonal structural phase transition and classical to quantum paraelectric phase transition in STO have been examined in the context. Also we have discussed some experimental techniques to study the phase transitions. We have shown the concept of using the order parameter, which has been implemented by Landau to describe the general behavior of the system. In principle, minimizing the free energy with respect to the order parameter can characterize the behavior of any system undergoes phase transitions.
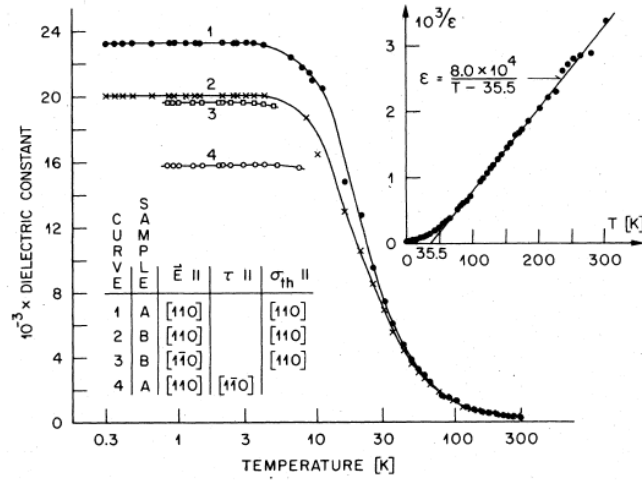
Figure 6: Dielectric constant ϵ_{110} and $\epsilon_{1\bar{1}0}$ of single domain STO.

References

[1] K. A. Muller, W. Berlinger, and E. Tossati, Z. Phys. B 84,277 (1991).

[2] E. D. Mishina, A. I. Morozov, and A. S. Sigov, J. Expe. Theo. Phys, Vol.94 No.3 pp 552-567 (2002)

[3] Y. P. Cai, D. Z. Han, and R. Y. Ning, J. Chem. Phys. Vol.23. No.2 (2009)

[4] K. A. Muller, H. Burkard, Phys. Rev. B19, 3593 (1979)

[5] G. J. Conduit, B. B. Simons, Phys. Rev. B 81, 024102 (2010)

[6] R. Mizaras, A.Loidl, Rhys. Rev. B 56, 10726 (1997)

[7] J. F. Scott, H. Ledbetter, Z. Phys.B 104, 635-639 (1997)